

# APEX-MR: Multi-Robot Asynchronous Planning and Execution for Cooperative Assembly

Philip Huang<sup>\*,1</sup>, Ruixuan Liu<sup>\*,1</sup>, Shobhit Aggarwal<sup>1</sup>, Changliu Liu<sup>1</sup> and Jiaoyang Li<sup>1</sup>

<sup>\*</sup>Equal Contribution, <sup>1</sup>Carnegie Mellon University

**Abstract**—Compared to a single-robot workstation, a multi-robot system offers several advantages: 1) it expands the system’s workspace, 2) improves task efficiency, and more importantly, 3) enables robots to achieve significantly more complex and dexterous tasks, such as cooperative assembly. However, coordinating the tasks and motions of multiple robots is challenging due to issues, *e.g.*, system uncertainty, task efficiency, algorithm scalability, and safety concerns. To address these challenges, this paper studies multi-robot coordination and proposes APEX-MR, an asynchronous planning and execution framework designed to safely and efficiently coordinate multiple robots to achieve cooperative assembly, *e.g.*, LEGO assembly. In particular, APEX-MR provides a systematic approach to post-process multi-robot tasks and motion plans to enable robust asynchronous execution under uncertainty. Experimental results demonstrate that APEX-MR can significantly speed up the execution time of many long-horizon LEGO assembly tasks by 48% compared to sequential planning and 36% compared to synchronous planning on average. To further demonstrate the performance, we deploy APEX-MR to a dual-arm system to perform physical LEGO assembly. To our knowledge, this is the *first* robotic system capable of performing customized LEGO assembly using commercial LEGO bricks. The experiment results demonstrate that the dual-arm system, with APEX-MR, can safely coordinate robot motions, efficiently collaborate, and construct complex LEGO structures.

## I. INTRODUCTION

Multi-robot manipulation is critical in robotic applications, such as industrial assembly [37, 3], material handling [50], and object arrangement [12, 14], etc. Compared to a single-robot setup, a multi-robot arm system can easily expand the system’s overall reachable area. Besides, with a team of robot arms, a task can be accomplished more efficiently [49] by having each robot execute individual tasks parallelly. In addition to improving task efficiency, multi-robot can achieve significantly greater dexterity and is *necessary* in many applications that require collaborations, *e.g.*, cooperative assembly, since certain tasks cannot be done with only one arm.

LEGO assembly is an example of cooperative assembly. In a LEGO structure, bricks are assembled by forcing the top knobs of a brick into the bottom cavities of another brick. The bricks are held together passively, *i.e.*, by the friction in the knob-to-cavity connections. Thus, the connections are not rigid, and subsequent manipulation, if performed inappropriately, can easily break the existing structure. Due to the nature of the passive connection, a multi-robot system is necessary for such cooperative assembly. Fig. 1 demonstrates example assembly operations in constructing a LEGO structure. Fig. 1(a) shows the robot picking up a brick by disassembling it from the LEGO plate (*i.e.*, pick). Fig. 1(b) illustrates the robot as-

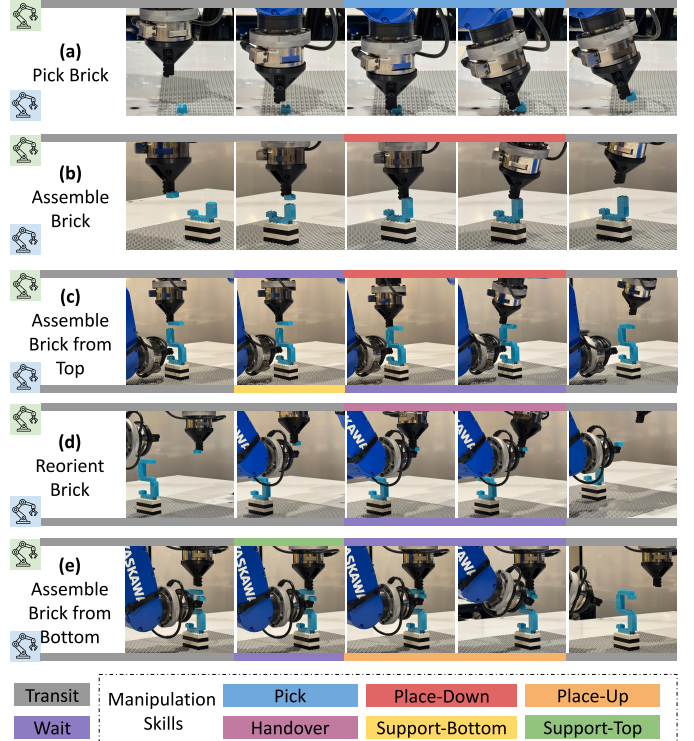


Fig. 1: Illustrations of bimodal cooperative assembly. Manipulation skills denote contact-rich operations for assembly.

sembling a brick by placing it at the desired location and forcing a solid connection (*i.e.*, place-down). One robot is sufficient for these two tasks since the manipulated object is fully supported and the operation would not collapse the existing structure. On the other hand, Fig. 1(c)-(e) showcase operations that require multi-arm collaboration. In Fig. 1(c), the upper robot is assembling a LEGO brick on top of the character ‘S’. To establish a solid connection, the robot needs to press down and force the knob insertion due to the passive connection nature. However, since the existing connections are non-rigid, the place-down operation would break the existing overhanging structure. Therefore, the lower robot is necessary to support and stabilize the structure from below (*i.e.*, support-bottom). Similarly in Fig. 1(e), the lower robot assembles a brick from the bottom onto the character ‘S’ by pushing it up and forcing the connection (*i.e.*, place-up). The place-up operation would break the existing structure, and thus, the upper robot is required to press down (*i.e.*, support-top)

in order to stabilize the structure. In addition to cooperative assembling, the multi-robot collaboration also enables more dexterous object manipulation, *e.g.*, reorienting bricks in hand. As shown in Fig. 1(d), the upper robot grabs a brick from its top initially. To have the robot grab the brick from its bottom, we can have the upper robot handover the brick to the lower robot. With the capability of reorienting in-hand objects, the robot can subsequently accomplish the assembly from the bottom as illustrated in Fig. 1(e). Despite being a toy brand, LEGO has been widely used in entertainment, education, prototyping, etc. It is ideal for assembly benchmarking since it is a low-cost, standardized, and highly customizable assembly platform. Meanwhile, constructing LEGO structures is a challenging contact-rich manipulation problem due to the high-precision requirement and non-rigid connections. Thus, we use LEGO as our cooperative assembly benchmarking platform and the remaining discussion is in the context of LEGO assembly.

Coordinating the tasks and motions of multiple robots to accomplish cooperative assembly is challenging for several reasons. First, a system with more than a single robot introduces overhead and algorithmic challenges in their coordination. As shown in Fig. 1 certain operations involve contacts with objects (*i.e.*, pick, place-down, place-up, handover, support-bottom, and support-top) while some do not (*i.e.*, transit and wait). There exist delays in controlling the robot and receiving sensor feedback, or even contingencies due to unexpected events when performing contact-rich operations, which would cause delays or stops to one or more robots. The uncertainty makes it challenging to safely coordinate the robots throughout the assembly process. Second, due to the collaboration need, robots often need to operate closely to each other as illustrated in Fig. 1(c)-(e). Even when executing under uncertainty in a confined shared workspace, robots must always avoid collisions. Third, it is desired that the task can be accomplished more efficiently by a multi-robot system. Thus, robots must have a comprehensive understanding of the cooperative assembly task and plan optimized motions to reduce the completion time, instead of frequently stopping to avoid collisions. Lastly, the multi-robot system should scale as the complexity of assembly design increases. It is necessary that the algorithm can scale to larger and more complex tasks.

Many recent works have proposed methods for planning multiple robot arms for assembly [22, 5], rearrangement [12, 13], or general manipulation tasks [45]. However, these planners often assume a sequential execution order and synchronously moving robots, where all robots start a task at the same time and wait for other robots to finish. We take a different lens and propose APEX-MR, an *asynchronous* planning and execution framework, to robustly, efficiently, and safely coordinate multiple robots. Given an assembly task sequence, APEX-MR leverages integer-linear programming (ILP) to distribute the tasks to the robots and generate a sequential robot plan. Most importantly, APEX-MR extends the temporal plan graph (TPG) [20] to multi-robot-arm systems and post-processes the sequential robot plan for

asynchronous execution. Specifically, the TPG captures all dependencies between different robots' tasks and motions and generates a partial-order graph, which can significantly reduce unnecessary wait time and is robust to execution delay and uncertainty. To highlight the applicability of our proposed algorithm within a full multi-robot assembly pipeline, we deploy the proposed APEX-MR to a dual-industrial-arm system to construct complex customized LEGO structures up to 258 objects in simulation and up to 47 objects in the real world. In summary, our contributions are as follows:

- We extend the TPG execution framework to multiple robot arms and show that it enables robust and safe multi-robot asynchronous execution under uncertainty.
- We propose a sequential multi-robot task and motion framework that is complementary to the TPG execution.
- We demonstrate algorithm deployment and system integration for bimanual LEGO assembly. To our knowledge, this is the *first* robotic system that can accomplish flexible (*i.e.*, customized complex designs instead of simple pick and stack) assembly using commercial LEGO bricks.

The rest of this paper is organized as follows: Sec. II discusses relevant works. Sec. III deliberates the input that APEX-MR consumes and assumptions we have. Sec. IV introduces our proposed APEX-MR, an asynchronous planning and execution framework for multi-robot cooperative assembly. Sec. V shows the experiment results and demonstrates the deployment to a bimanual system for LEGO assembly. Sec. VI discusses limitations and future works. Sec. VII concludes the paper.

## II. RELATED WORKS

**Multi-Robot Arm Motion Planning** Motivated by the rise of bimanual manipulation systems, many early works in the field study the problem of dual arm motion planning [51]. One naive approach that scales single-robot motion planning methods to two or more robots is to plan in the composite joint space, with methods such as RRT-Connect [25], BIT\* [11], or graph of convex sets [35]. However, due to the curse of dimensionality, these methods struggle to find high-quality solutions as the number of robots increases. Other common strategies include building a composite roadmap from the Cartesian product of individual roadmaps [15], coordinating the speed of individually planned motions [2], or using prioritized planning [8]. More recently, more specialized multi-robot motion planners have been proposed that are based on roadmaps (dRRT [53], dRRT\* [48], and CBS-MP [52]) or utilizing multi-agent path finding techniques [44, 45]. Some approaches also use online planning or control techniques to generate motions in real-time. Zhang and Pecora [61] proposes an online motion coordination technique, in which they plan all robot's paths offline and a pairwise collision matrix between robots. Then, the speed of each robot can be efficiently planned online to avoid collisions, even in the presence of execution delays. However, their method cannot always find a feasible motion and relies on a task reallocation process to avoid deadlock. Other techniques such as a distributed model predictive controller [10] or a dynamical system approach [38]

can also be used to generate multi-robot arm motions in real-time, but are not tailored towards long-horizon planning tasks.

**Multi-Robot Task and Motion Planning** Beyond motion planning, multi-robot arm task and motion planning (MR-TAMP) have been studied since the 1990s, *e.g.*, object pick and place [24], and many of which are designed for a dual arm setting [17, 12, 14, 51]. Similar to our method, these methods take a two-staged approach in which they first generate a task plan with robot assignment and grasp poses, then search for corresponding motion plans with composite-state-space or prioritized planning. The authors of dRRT\* have proposed extending dRRT\* to multi-modal roadmaps with given possible pick-up and hand-off configurations and searching for a task and motion plan directly [47, 46]. Given that motion planning calls tend to be more costly, another approach is to generate promising task plans first in a lazy manner and subsequently find corresponding motion plans and backtrack when required. This approach can be implemented with a greedy method [18], with a mixed-integer linear program [49, 5, 31] or through a satisfiability modulo theories solver [42]. However, a major drawback is that task planning often assumes motions to be synchronous, which can be suboptimal in practice. Our TPG framework is designed to be complementary to these synchronous tasks and motion planners, as it can relax the synchronicity assumption with post-processing and shorten the makespan of the overall plan. Another significant concern is that many MR-TAMP methods are designed for simple environments such as object pick and place and planned robot trajectories are executed in open-loop or only in simulation. Our framework scales to more complex environments and is designed to integrate with more challenging manipulation skills such as a force-feedback controller.

**Multi-Robot Arm Motion Execution** Most existing work executes their multi-robot on real robots in a synchronized way. Since the popular motion planning framework *MoveIt!* [7] does not natively support moving multiple robot arms asynchronously, some recent work have sought to address this and enable asynchronous execution. Meehan et al. [36] adds a trajectory reservation component and treats the entire trajectory of a moving robot arm as a static obstacle when planning another arm’s motion, which can be too conservative and cause deadlock. Stoop et al. [55] uses a central scheduler to check if a new trajectory collides with previously scheduled trajectories and executes it asynchronously if there is no collision. Otherwise, the new trajectory waits for the conflicting previous trajectory to finish before it can start. However, their methods do not account for execution delays, may wait longer than necessary, and directly modify the *MoveIt!* software stack. In contrast, our TPG formulation is robust to arbitrary delays by design, minimizes robot wait time, and can be implemented without modification to *MoveIt!*.

**Multi-Agent Path Finding and Execution** Multi-agent path finding (MAPF) [54] studies how to coordinate a large team of mobile robots in a discretized world environment, often on 2d grid worlds representing warehouse settings [32] or pre-defined roadmaps [21]. State-of-the-art MAPF algo-

rithms can plan near-optimal collision-free paths for hundreds of robots in seconds [26].

However, these MAPF algorithms achieve such impressive efficiency at the cost of neglecting robot kinematics and execution uncertainty. As a result, there is growing research within the MAPF community focused on the efficient and robust execution of (imperfect) MAPF plans on real robots. One of the most widely adopted frameworks is the temporal plan graph (TPG) [20], originally proposed to post-process MAPF plans to meet robot kinematics by enforcing passing orders at locations visited by multiple robots. TPG has since been extended to execution frameworks for MAPF under uncertainty [33] and mobile robot coordination in warehouses [19, 59]. Recent advancements introduce bidirectional TPG [56] and switchable TPG [1, 23], which further enhance TPG by allowing flexible passing orders at certain locations.

Given the success of TPG in coordinating mobile robots, we aim to explore its applicability in coordinating robotic arms. A key distinction of traditional TPG versus our use case is that the robot kinematic is more complex, and may change over time as the robot arm picks up different object, which is a key focus in this paper.

**Robotic LEGO Assembly** Automating LEGO assembly using robots is challenging due to the high-precision requirement, tiny sizes of LEGO bricks, and non-rigid connections in the structure. Most of the existing works address the LEGO assembly problem in simulation [43, 39], which cannot be generalized to physical assembly due to the lack of simulators to simulate the connections between LEGO bricks. Recent works [9, 16, 27, 30] assume the structure is fully supported and only consider placing bricks on top of others, which are limited to assembling simple structures. [34] considers assembly using customized brick toys, which does not apply to LEGO assembly. In this paper, we apply APEX-MR to a bimanual system to construct complex customized LEGO structures beyond simple stacking.

### III. PRELIMINARIES

To coordinate a multi-robot system to perform cooperative assembly tasks, we assume three inputs are provided.

**Environment Setup** We assume the environment setup, including (a) geometries of all robots, (b) poses of objects to be manipulated  $\mathcal{B} = [b_1, b_2, \dots, b_{N_b}]$ , and (c) states of all obstacles, is known as shown in the input section in Fig. 2. We assume the system consists of  $N$  robots, and  $N_b$  is the number of objects that can be used for the assembly. An object  $b_i$  is semi-static, meaning it can be grasped, attached, and moved by the robots. Note that since duplicate objects are common in assemblies,  $b_i$  and  $b_j$  can be identical objects, *e.g.*, identical  $2 \times 2$  bricks in the character ‘S’ shown in Fig. 2.

**Assembly Plan** Given an assembly design with  $N_a$  objects, we assume the assembly plan  $A = [a_1, a_2, \dots, a_{N_a}]$  is provided as shown in the input section in Fig. 2. Each step  $a_j$  refers to an object, such as a  $1 \times 2$  brick. The assembly plan specifies the order in which each object should be assembled.

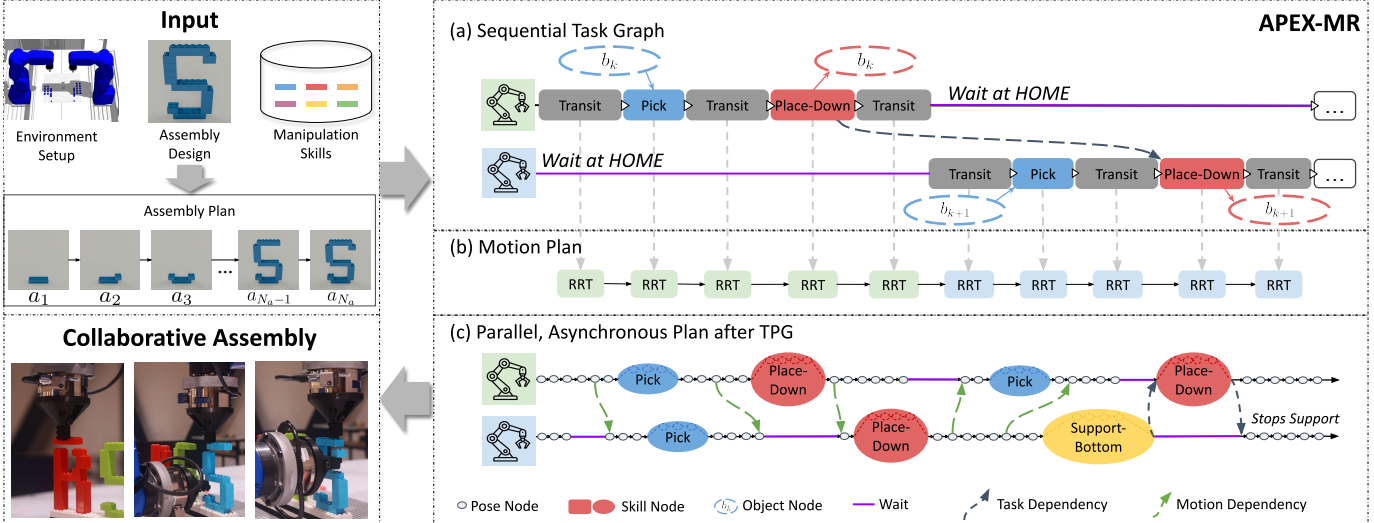


Fig. 2: An overview of APEX-MR. On a high level, APEX-MR builds a sequential task plan given an assembly sequence, plans the motion of each task with RRT-Connect, and converts the solution to a parallel, asynchronous plan for execution with a TPG. Specifically, (a) shows the example of a task graph, (b) illustrates generating robot motion from the task plan, and (c) shows the example of a multi-modal TPG.

Note that due to duplicate objects in  $\mathcal{B}$ , there are multiple candidates  $b_i, \dots, b_k$  that can be used to accomplish an assembly step  $a_j$  in  $A$ . Furthermore, we require the assembly plan  $A$  to be physically valid [58, 28], ensuring that each task can be performed in reality. Specifically, the partially assembled structure after each step  $a_j$  must be physically stable, and there exists at least one feasible grasp pose for each step. The assembly sequence also specifies whether each step  $a_j$  requires two robots for cooperative assembly and the specific type of cooperation needed (*i.e.*, support or reorientation). Lastly, we assume  $\mathcal{B}$  is sufficient so that each object required for  $a_j$  can be found in the environment, *i.e.*,  $A \subseteq \mathcal{B}$ .

**Manipulation Skills** We assume that the robot manipulation skills are predefined and known. We denote the skill set as  $\mathcal{S} = [s_1, s_2, \dots, s_{N_s}]$ , where  $N_s$  is the number of skills an individual robot has. For instance, a skill can be, inserting a pin, fastening a screw, picking up an object, etc. In our case of LEGO assembly, each skill  $s_i$  is a composite of multiple motions parametrized by the pose of the manipulated object, the robot end-effector, and parameters learned from demonstrations. We assume an algorithm, such as interpolation or RRT-Connect, can generate a reference robot trajectory for the purpose of computing a collision-free coordination schedule. During execution, each skill is executed with a feedback controller so that its exact execution time is unpredictable. Example manipulation skills are shown in Fig. 1, and more details are discussed in Sec. V.

In addition to these inputs, we assume the existence of a collision-free HOME pose for each robot that never blocks other moving robots from executing their tasks. Robots can also transit between different poses, or wait and hold their current pose in place.

#### IV. APEX-MR: ASYNCHRONOUS PLANNING AND EXECUTION FOR MULTI-ROBOT SYSTEM

In this section, we introduce APEX-MR, a framework for asynchronously coordinating the task plan, motion, and execution of a multi-robot system to accomplish cooperative assembly tasks. Fig. 2 provides an overview of the three stages of APEX-MR. Given the input discussed in Sec. III, a sequential task plan and the corresponding task graph, as shown in Fig. 2 (a), are generated from the assembly using ILP. The motion plan for each task is then generated sequentially with a single-robot motion planner (see Fig. 2 (b)). The last and most crucial step, Fig. 2 (c), converts the sequential plan to a multi-modal TPG that can be executed safely, asynchronously, and efficiently in real.

We will present these algorithmic components in order in the following discussion. For notations, we use  $i \in [1, N]$  to index over robots,  $j \in [1, N_a]$  to index over assembly steps in  $A$ ,  $m$  to index over tasks for each robot, and  $k \in [1, N_b]$  to index over usable objects in  $\mathcal{B}$ .

##### A. Task Planning

Given the assembly sequence  $A$ , task planning aims to construct a sequential task plan that includes robot assignment, robot target pose assignment, and object assignment. Specifically, for each step  $a_j$  in the assembly sequence, the task planner must assign one responsible robot, a support robot if required, and an object  $b_k$  of the correct type. In addition, the task planner must select the feasible grasp pose, or a composite motion of multiple poses, to perform necessary manipulation skills for each  $a_j$ . Fig. 3 provides an overview of all the decisions made. These decisions directly affect the feasibility of motion planning, as task planning determines whether there are collision-free and deadlock-free paths.

**Task Definition** We define a task  $\mathcal{T}^i$  as a piece of work that requires robot  $i$  to either transit to a goal pose or to perform some manipulation skill  $s$  to achieve a goal constraint. For example, a task may involve a robot arm picking up an object, supporting a structure, receiving an object handed from another robot, retracting to its HOME pose, etc. In the context of LEGO assembly, each assembly task  $a_j$  is broken down into a sequence of tasks. As shown in Fig. 1 (a) and (b), a robot must first transit to the initial location of an object, pick the object, transit the object to the location for assembly, place down the object on the target structure, and finally transit back to the robot’s HOME. For an assembly step that requires collaborative assembly, the support robot is also assigned a sequence of tasks, such as transiting to the structure and supporting it in Fig. 1 (c) and (e). If a reorientation is required as illustrated in Fig. 1 (d), the support robot will be assigned a transit and a pick task to collect the object, and a handover task to the other robot so that the object can be placed up to the structure.

**Task Graph** A task graph  $\mathcal{G} = (\mathcal{V}, \mathcal{E})$  is a direct acyclic graph that represents the ordered set of tasks for all robots to complete the final assembly. The task graph also implicitly represents the movement of manipulated objects, the evolving environment and collision scene, as well as the kinematic switches of the robots. A node is either a task node or an object node. A task node represents a task  $\mathcal{T}_m^i \in \mathcal{V}$  for robot  $i$ , where  $m$  is the index. Each task node also contains a robot target pose for this task. An object node represents an object  $b_k$  and its poses. An edge from one task node to another in the graph,  $\mathcal{T}_m^i \rightarrow \mathcal{T}_{m'}^{i'}$ , represents a precedence constraint, that states a dependency where  $\mathcal{T}_m^i$  must be executed before  $\mathcal{T}_{m'}^{i'}$  can start. An edge from an object node to a task node,  $b_k \rightarrow \mathcal{T}_m^i$ , means that the object  $b_k$  is kinematically attached to the robot  $i$  at the beginning of this task. In contrast, an edge from a task node to an object node,  $\mathcal{T}_m^i \rightarrow b_k$ , represents that an object would be detached from robot  $i$  after this task ends. Each robot  $i$  has  $M^i$  tasks. A task graph itself does not limit if the tasks must be executed sequentially, synchronously, or asynchronously.

**Approach** The main idea of our approach is to find a turn-based, sequential task plan according to the assembly sequence  $A$ , which is itself sequential. Only one robot is actively moving or executing skills at any time, while the other robot waits. Each robot returns to its HOME pose at the end of completing an assembly step.

Algorithmically, an ILP jointly optimizes robot assignment, object assignment, and target robot poses. A set of binary decision variables assigns a robot  $i$  to an assembly step  $a_j$  using the object  $b_k$  and a feasible grasp pose. Another set of binary decision variables denotes whether the assignment of support robot and support poses. We precompute feasible robot poses for grasping all available objects at initial and assembled positions, and support poses if necessary. The cost for assigning a robot  $i$ , an object  $b_k$ , and a corresponding grasp pose to an assembly step  $a_j$  is estimated by the sum of transit distances necessary for this assembly step. The ILP finds the best set of assignments that minimizes the sum of

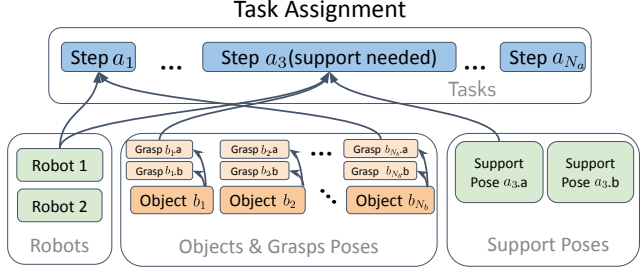


Fig. 3: An overview of the task planning in APEX-MR. Given the assembly sequence  $A$ , each step  $a_j$  is assigned a robot, an object, a feasible object grasp pose, and a supporting pose if necessary.

costs to complete the assembly and an auxiliary term for load balancing while ensuring the object type and support robot requirements are met. More details of the ILP formulation are discussed in appendix A.

Combined with the precomputed robot poses, the optimized assignment gives a complete set of robot, object, and grasp pose assignment in each step. We then construct a corresponding sequential task plan and task graph (e.g., Fig. 2 (a)) with all inter-robot task dependencies and object relationships. A sequence of tasks for the assigned robot is added for each assembly step, and two object nodes are added to the task graph and connected to the pick task and place task nodes to indicate their attachment and placement, respectively. If a collaborative assembly is required, then a sequence of support tasks is added to the support robot to be completed first. Inter-robot task dependencies are added to the task graph to constrain that the support task must precede any place task, and the following task after support can only start after the place task finishes. If two consecutive assembly steps  $a_j$  and  $a_{j+1}$  are assigned to different robots, a task dependency is added to ensure the place task for  $a_{j+1}$  must wait for the place task for  $a_j$ .

Compared to other MR-TAMP and assembly methods such as [14, 18, 42, 5], APEX-MR generates a sequential plan first. This has two advantages: (1) It is easy to reason about inter-robot collision for scheduling tasks and avoids expensive feasibility checks needed for parallel task execution; (2) The complexity of motion planning is significantly reduced since each task becomes a single-robot planning problem, which avoids solving a challenging and time-consuming multi-robot arm motion planning problem. It is worth noting that, while the sequential plan might seem inefficient for a multi-robot system, our execution step will post-process this plan to enable efficient parallel execution.

## B. Motion Planning

Once the sequential task plan for each robot is determined, motion planning becomes straightforward. As illustrated in Fig. 2 (b), APEX-MR iterates over each task and use a single-robot RRT-Connect algorithm to plan the trajectory for this task when other robots are waiting. This is feasible because all other robots would be at a nonblocking stationary

pose, *i.e.*, HOME. A reference trajectory is also generated for tasks executed by specific manipulation skills based on the grasp/support pose.

The motion planner generates a planned trajectory for every robot and every task. Each trajectory  $\tau_m^i$  for robot  $i$  and task  $\mathcal{T}_m^i$  is represented with a sequence of uniformly timestamped poses,  $\{(C_n^i, t_n^i)\}$ ,  $n \in [N_{start,m}^i, N_{end,m}^i]$  with step size  $\Delta t$ .  $N_{start,m}^i$  and  $N_{end,m}^i$  are the first and last index of the trajectory  $\tau_m^i$ ,  $N_{start,1}^i = 1$ , and  $N_{start,m+1}^i = N_{end,m}^i + 1$ . For each task, the planner first generates a sequence of poses  $C_n^i$  for the robot  $i$ , then determines corresponding timestep  $t_n^i$  for each pose based on the maximum velocity, *i.e.*,  $t_m^i = t_{n-1}^i + d(C_n^i, C_{n-1}^i)/v_{max}$ . The timing in the trajectory also ensures that each robot takes turns to complete its task according to the task sequence. Hence, the initial timestep of each task is equal to the last timestep of the previous task in the sequential task plan. Since RRT-Connect may produce jerky and long trajectory, we use a randomized shortcircuiting algorithm to smooth suboptimal trajectories. The output of motion planning should be a sequence of trajectories for each task, *i.e.*,  $\tau_m^i$ ,  $\forall i \in N$ ,  $\forall m \in M^i$ .

### C. Asynchronous Execution

From the sequential task and motion plan, APEX-MR converts it to a TPG to improve the quality of the plan and support asynchronous execution. Importantly, the process to construct a TPG is not limited to a sequential plan and also applies to synchronous plans commonly seen in MR-TAMP works such as [42, 46, 49].

**TPG Definition** APEX-MR uses a multi-modal temporal plan graph (TPG) to represent an execution schedule for the team of robot manipulators. As illustrated in Fig. 2 (c), multi-modal TPG is a directed acyclic graph  $G = (V, E)$  with two types of node. A pose node  $v_n^i$  corresponds to a configuration  $C_n^i$  on the trajectory of a transit task for robot  $i$ . A skill node  $\tilde{v}_n^i$  represents a manipulation skill (*e.g.*, pick, handover, support, etc) that will be executed by some robot controller or policy. The skill node also contains a reference trajectory generated in motion planning. A type-1 edge  $(v_n^i \rightarrow v_{n+1}^i)$  connects two nodes from the same robot  $i$  and indicates the order between two nodes. A type-2 edge  $(v_n^i \rightarrow v_{n'}^{i'})$  represents an inter-robot precedence order that constrains the robot  $i'$  to wait for robot  $i$  to reach the pose at  $C_n^i$  or finish the skill at  $v_n^i$  before moving to  $v_{n'}^{i'}$ . A type-2 edge can be added for both task dependencies and motion dependencies. In contrast to the TPG defined in [20], a multi-modal TPG combines a TPG with a task graph and assigns a corresponding task  $\mathcal{T}_m^i$  to each node  $v_n^i$ . Since there are kinematic switches and changes to the collision environment, each node also contains the robot kinematic (*i.e.*, attached object), which will be important for the TPG construction process.

**Building a multi-modal TPG** The process of constructing a TPG from a multi-robot motion plan can be interpreted as converting from the sequential robot trajectories to temporally dependent robot schedules. On a high level, inter-robot task dependencies are copied as type-2 edges for TPG, and type-2

---

### Algorithm 1 Multi-Modal TPG Construction

---

```

1:  $\triangleright$  Input: A task graph  $\mathcal{G}$  and all robot trajectories  $\tau_m^i$   $\triangleleft$ 
2: for robot  $i = 1, \dots, N$  do
3:   for task  $\mathcal{T}_m^i = \mathcal{T}_1^i, \dots, \mathcal{T}_{M^i}^i$  do
4:     if task  $\mathcal{T}_m^i$  is executed by a skill then
5:       Add a sequence nodes  $\{v_n^i\}$  from  $\tau^i$ 
6:       Add type-1 edges for consecutive nodes
7:     else Add a skill node  $\tilde{v}_n^i$ 
8:     Add type-1 edge from  $v_{N_{start,m}^i}^i$  to  $v_{N_{end,m}^i}^i$ 
9:   for task dependency  $(\mathcal{T}_m^i \rightarrow \mathcal{T}_{m'}^{i'}) \in \mathcal{E}$  such that  $i \neq i'$  do
10:    Add type-2 edge from  $v_{N_{start,m+1}^i}^i$  to  $v_{N_{start,m'}^{i'}}^{i'}$ 
11:   for robots  $(i, i') = \{1, \dots, N\} \otimes \{1, \dots, N\}$  do
12:     if  $i == i'$  then continue
13:      $\triangleright$  (Optional) parallelize the following  $\triangleleft$ 
14:     for  $n = 1, \dots, N_{end,M^i}^i$  do
15:       Update robot  $i$  kinematic if needed
16:       for  $n' = 1, \dots, N_{end,M^{i'}}^{i'}$  do
17:         Update robot  $i'$  kinematic if needed
18:         if  $t_{n'}^{i'} \geq t_n^i$  or  $v_n^i$  depends on  $v_{n'}^{i'}$  then
19:           continue
20:           if  $v_{n'}^{i'}$  collides with  $v_n^i$  then
21:             Add type-2 edge from  $v_{n'+1}^{i'}$  to  $v_n^i$ 
22:   Simplify TPG with transitive reduction.

```

---

edges for motion dependencies are constructed by scanning for collisions between all pair of TPG nodes. A key benefit of this partial-order representation is that TPG does not specify a fixed time between two consecutive nodes, and thus allows execution delays. We outline the detailed procedure below.

The construction process begins by creating the nodes and type-1 edges. For each transit task  $\mathcal{T}_m^i$ , a pose node  $v_n^i$  is constructed for each configuration  $C_n^i$  of the trajectory  $\tau_m^i$ . A skill node  $\tilde{v}_n^i$  is created for every manipulation task. The timestamp in the input trajectory  $t_n^i$  for each node  $v_n^i$  is also recorded. Each node  $v_n^i$  is then connected to its successor  $v_{n+1}^i$  by a type-1 edge, and the end node of a task  $v_{N_{end,m}^i}^i$  is connected to the start node of the next task  $v_{N_{start,m+1}^i}^i$ . When a robot waits at a node  $v_m^i$ , that is  $C_m^i = C_{m-1}^i$ , the node  $v_m^i$  is removed. This is because removing wait action does not change the robot path or any temporal dependency in the TPG.

Next, all the type-2 edges are identified the TPG. First, all inter-robot task dependencies  $(\mathcal{T}_m^i \rightarrow \mathcal{T}_{m'}^{i'}) \in \mathcal{E}$  from the task graph  $\mathcal{G}$  are added as type-2 edges to the TPG. Specifically, for every edge in the task graph  $\mathcal{T}_m^i \rightarrow \mathcal{T}_{m'}^{i'}$ , a type-2 edge is added from the beginning of task  $\mathcal{T}_{m+1}^i$ , *i.e.*, node  $v_{N_{start,m+1}^i}^i$ , to the beginning of task  $\mathcal{T}_{m'}^{i'}$ , *i.e.*, node  $v_{N_{start,m'}^{i'}}^{i'}$ . This type-2 edge ensures that robot  $i$  only starts  $\mathcal{T}_{m'}^{i'}$  after robot  $i'$  finishes executing task  $\mathcal{T}_m^i$ .

Then, motion-level dependencies are identified by iterating over all pairs of nodes in the TPG with a double loop iterating over  $(i, i')$ . Robot kinematics can be incrementally changed if

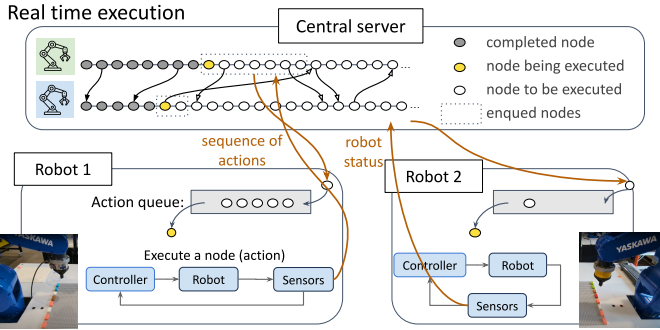


Fig. 4: Illustration of the execution setup. TPG maintains and controls the execution schedule of all robots on a central server, gradually sending new trajectory segments that can be safely executed. Each robot maintains a controller-sensing loop independently while updating its state with the central server.

node  $v_n^i$  is the start of a new task that attaches or detaches an object. For each node  $v_n^i$ , it is checked against all other nodes  $v_{n'}^{i'}$  from a different robot ( $i \neq i'$ ) and has an earlier timestamp  $t_{n'}^{i'} \leq t_n^i$ . Collision checking for pose nodes means that the robot links and attached objects at the corresponding poses  $C_n^i$  and  $C_{n'}^{i'}$  are checked. For skill nodes, all robot poses on the reference trajectory have to be collision-free simultaneously. If there is any collision between  $v_{n'}^{i'}$  and  $v_n^i$ , a type-2 edge is added from the earlier node's successor,  $v_{n'+1}^i$ , to the later node,  $v_n^i$ . This way, if  $v_{n'}^{i'}$  is executed before  $v_n^i$  in the input sequential plan,  $v_{n'}^{i'}$  must still be executed before  $v_n^i$  can start, avoiding any potential collisions. When iterating  $n'$ , it is unnecessary to check collisions for any node  $v_{n'}^{i'}$  that has a larger timestamp than  $v_n^i$ , *i.e.*,  $t_{n'}^{i'} \geq t_n^i$ , because those would be checked when the iterated robot pair ( $i, i'$ ) are swapped. Also, if the current  $v_{n'}^{i'}$  is a predecessor of  $v_n^i$  in the graph,  $v_n^i$  already waits for  $v_{n'}^{i'}$  and avoid collisions, so it becomes unnecessary to check them again.

The total number of collision checks needed depends on the number of robots, discretized steps, and type-2 edges added from the task graph. Once every node has been checked against potentially colliding nodes, a transition reduction algorithm is applied, similar to [33] to simplify the TPG. A type-2 edge  $v_n^i \rightarrow v_{n'}^{i'}$  is redundant if node  $v_n^i$  is still a predecessor of node  $v_{n'}^{i'}$  after the edge is removed. We remove all such redundant edges to reduce the total number of scheduling constraints and communication overheads during execution.

The primary bottleneck of the TPG construction process is the number of collision checks, which scales quadratically with respect to the number of robots and the number of nodes. To alleviate this, collision checking can be parallelized across many CPU threads, reducing its runtime. A pseudocode of the entire construction process is provided in Algo. 1.

**Further Optimization** An optional step to further reduce the execution makespan and smooth the trajectory is to skip the intermediate transition to HOME after every assembly step. We use the following shortcutting algorithm, similar to the strategy implemented in [41], to achieve that while maintaining

a collision- and deadlock-free plan.

The anytime algorithm works by randomly sampling two nodes of the TPG ( $v_n^i, v_{n'}^{i'}$ ) from the same transit task  $T_m^i$ , checking whether connecting them in a shortcut is feasible. Consecutive transit tasks passing through the robot's HOME pose are merged as a single task. This allows the HOME pose to be skipped. A shortcut path directly interpolates between  $C_n^i$  and  $C_{n'}^{i'}$  to generate a sequence of poses with the same step size  $\Delta t$ . The shortcut must be collision-checked against any independent nodes (*i.e.*, nodes that are not predecessors or successors of  $v_m^i$  or successors to  $v_{m'}^{i'}$  in the TPG). On a multi-modal TPG, the collision checking must include any attached objects to the robot, as well as any independent object nodes on a task graph (*i.e.*, object nodes that are not predecessors or successors of the current task). Once a valid shortcut is found, the original nodes between  $v_m^i, v_{m'}^{i'}$  are replaced with new nodes corresponding to the shortcut. If adding a valid shortcut from  $v_n^i$  to  $v_{n'}^{i'}$  skips any outgoing edges between these two nodes, the start node of these outgoing edges is moved to  $v_n^i$ . If any incoming edges are skipped, then the start node of these incoming edges is moved to  $v_{n'}^{i'}$ . This ensures that any dependencies before adding a shortcut still exist after, and the TPG remains collision-free. Since each shortcut is collision-free, no new dependencies in the TPG are introduced and TPG remains deadlock-free. The shortcutting algorithm keeps identifying valid shortcuts until a user-defined time limit is reached, removing redundant transitions to HOME poses in the process.

#### D. TPG Execution

Executing a motion plan on robot arms often requires a position controller for movement and other specific controllers for manipulation skills. These controllers may have delays or uncertainties that affect the real-robot execution time. The TPG formulation provides an easy way to execute a multi-robot plan. Here, we present one centralized mechanism to coordinate multiple robot arms.

As shown in Fig. 4, the TPG is hosted on a central server that communicates with each robot's execution thread. Each pose node in the TPG corresponds to an action that moves the robot's position to the node's configuration. Each skill node corresponds to an action that executes the predefined robot skill. An action can be safely executed if there are no incoming edges from any nodes that are not executed.

If an action is safe to execute based on the TPG, the central server sends it to the robot's action queue. Each robot maintains its own controller-sensing loop and controls the robot according to upcoming commands and its state estimation. The state estimation is also shared with the TPG, which then updates the TPG when a node is being executed or completed. Newly completed nodes may also allow new nodes to be queued if their outgoing edges were previously preventing unsafe actions. During execution, TPG can be interpreted as a control law that maintains the safe scheduling of individual robot actions.

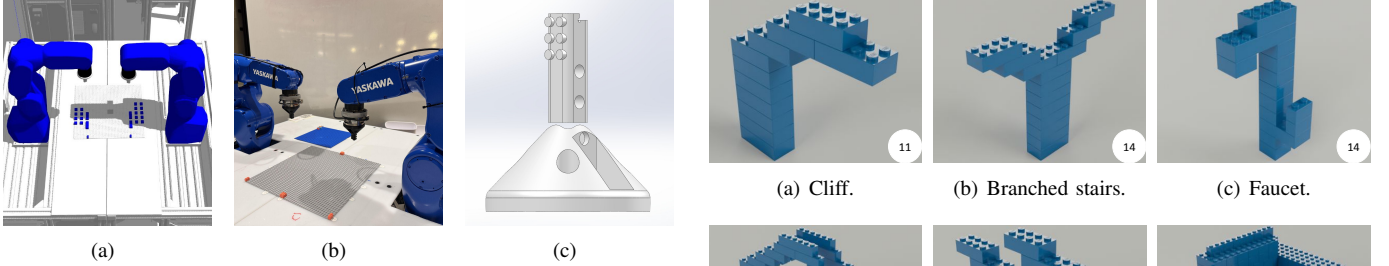


Fig. 5: Experiment setup for bimanual LEGO assembly. (a) Simulation environment. (b) Real setup. (c) Illustration of the EOAT, *i.e.*, LT-V2, for the robot to construct LEGO structures.

## V. RESULTS

To evaluate the performance, we apply the proposed APEX-MR to bimanual LEGO assembly tasks. Given a customized LEGO design as shown in Fig. 6, APEX-MR coordinates the robots to construct the desired structure as shown in Fig. 9 using available LEGO bricks. We deliberate the inputs (introduced in Sec. III) to APEX-MR below.

**Environment Setup** Figure. 5(a) and 5(b) illustrate the simulation environment and the real setup, which includes two Yaskawa GP4 robots. Following the task convention in [30], we consider building LEGO structures on a baseplate, which is calibrated<sup>1</sup> and placed in between the two robots, using commercial standard LEGO bricks initially stored on the baseplate. Each robot is equipped with an ATI Gamma force-torque sensor (FTS) and the end-of-arm tool (EOAT) is mounted on the FTS. The simulation consists of the entire workspace, which includes the robots, FTS, EOAT, LEGOs, nearby workstations, etc. The complete digital environment provides rich and accurate information for APEX-MR to safely coordinate the robot collaboration.

**Assembly Plan** Given a LEGO structure, we employ the physics-aware assembly planning in [28] with customized LEGO physics reasoning [29] to generate a physically valid assembly sequence. Specifically, a physically valid assembly sequence enforces that for each step after assembling a brick, the structure is stable and does not collapse. Note that the definition of a physically valid assembly sequence can be different for other cooperative assembly tasks. For other applications, the assembly sequence can be obtained via planners, *e.g.*, [58], and the proposed APEX-MR is also applicable downstream.

**Manipulation Skills** Manipulating LEGO bricks is a non-trivial contact-rich manipulation problem beyond simple pick and stack. A robot EOAT and manipulation policy (*i.e.*, insert-and-twist) was presented in [30], which enables a robot to manipulate commercial standard LEGO bricks, *i.e.*, pick, and place-down in Fig. 1. However, a robot can only use it to manipulate a LEGO brick from its top, which limits the system from constructing complex structures. To enhance the system capability, we present a new LEGO tool (LT-V2), as shown

<sup>1</sup>We calibrate the transformation from the robots to the baseplate by teleoperating the robot to touch the plate. Note that we only measure the translation ( $X$ ,  $Y$ ,  $Z$ ) and yaw angle while assuming no roll and pitch offsets.

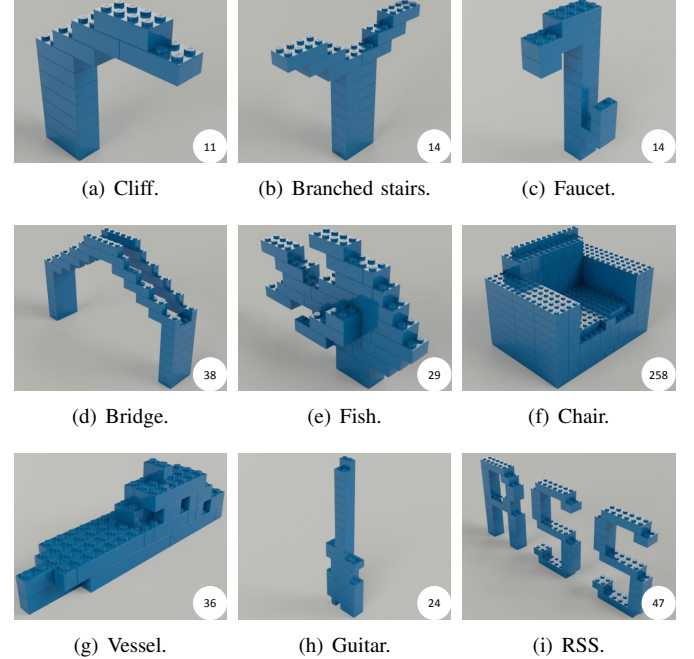


Fig. 6: Customized LEGO designs for evaluating APEX-MR. The number in each figure indicates the number of objects required to assemble the LEGO structure.

in Fig. 5(c). In particular, LT-V2 has LEGO studs added to the side of the tooltip. The new design enables the robot to manipulate a brick from its bottom as shown in Fig. 1, *i.e.*, handover and place-up. With LT-V2, we define the manipulation skills as shown in Fig. 1, including 1) goal reaching with force feedback (*i.e.*, support-bottom and support-top), and 2) learned force policy (*i.e.*, pick, place-down, place-up, handover). For each skill, we generate a maximum of one feasible (*i.e.*,  $G = 1$ ) LEGO grasp pose and one support pose if necessary to use in task planning.

**Implementation** We implement the TPG algorithm and manipulation skills in C++ with ROS-Noetic and *MoveIt!* [7]. The ILP in task planning is solved with the pulp Python package. The RRT-Connect motion planning uses *MoveIt!*'s OMPL [57] plug-in. Trajectories are discretized using  $\Delta t = 0.05$  when the maximum  $L_1$  joint velocity is 1 rad/s.  $\Delta t$  is adjusted linearly based on the max velocity to ensure the same density. All simulation experiments are conducted on an AMD 7840HS laptop.

**Experiment Objective** While APEX-MR itself is a full pipeline for multi-robot tasks and motion planning, the key innovation that enables asynchronous innovation is the TPG execution framework. Thus, we are interested in the following questions when evaluating APEX-MR:

- (Q1) How significant is the benefit of asynchronous execution, enabled by the TPG execution framework?
- (Q2) How is the quality of plans produced by APEX-MR and what are the computational costs?
- (Q3) How well does APEX-MR on physical LEGO assembly and can it safely execute planned trajectories

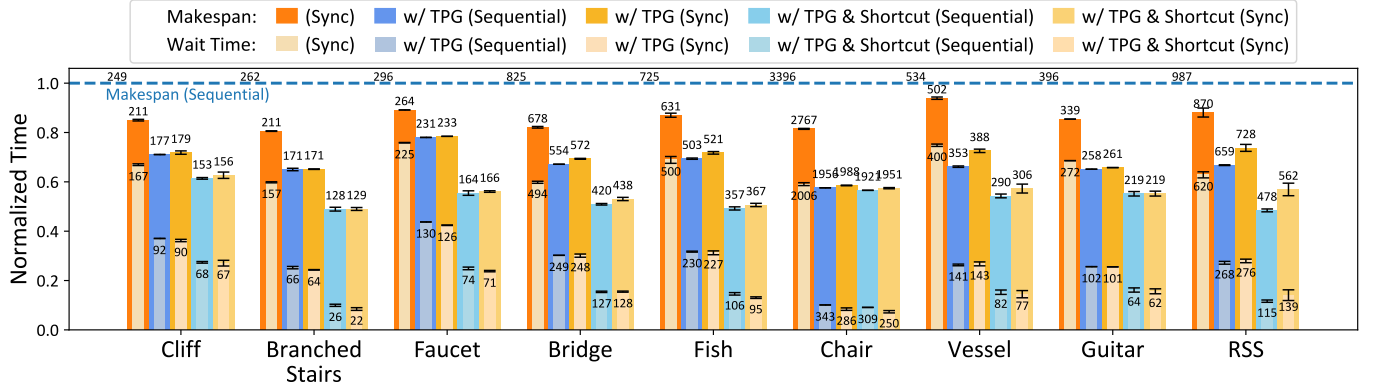


Fig. 7: Normalized makespan and wait time of APEX-MR (Sequential) versus the synchronized planner across example evaluation environment. The results are normalized by the makespan of the sequential motion plan before TPG and averaged over 4 random seeds. The unnormalized makespan and wait time are labeled for each entry and the dashed horizontal line corresponds to the makespan of the sequential motion plan before TPG.

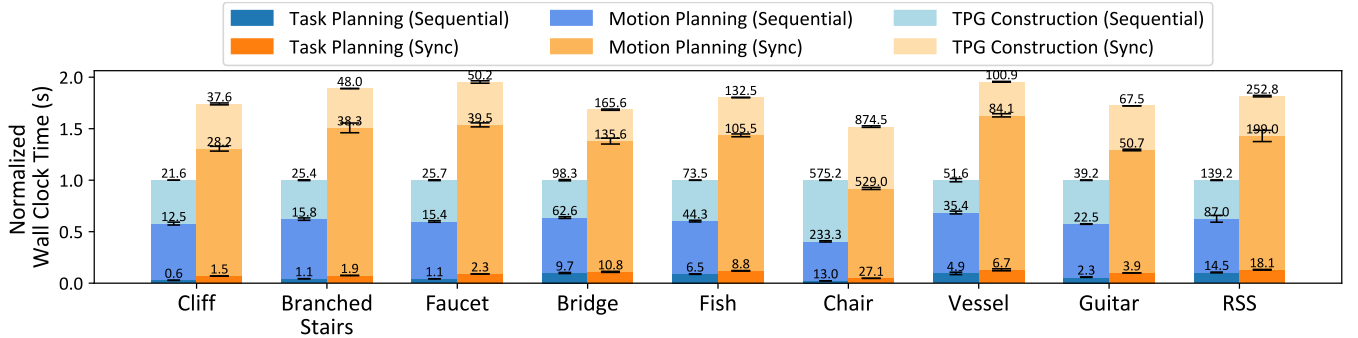


Fig. 8: Breakdown of wall clock time of APEX-MR (Sequential) and the synchronized planner baseline across evaluation environments. The results are normalized by the total of APEX-MR planning time for each task (excluding shortcutting) and averaged over 4 random seeds. The running sum of unnormalized wall clock time is labeled for each component.

despite uncertainties?

Q1 and Q2 will be examined closely in simulation, whereas Q3 will be the focus of our real robot experiments.

#### A. Simulation Performance

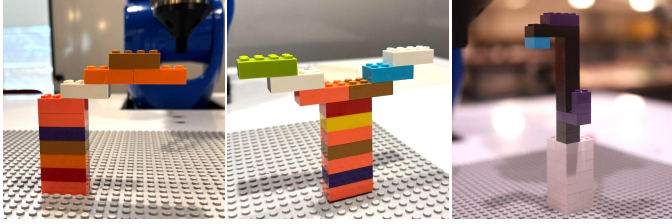
We first conduct experiments in simulation. To our knowledge, no existing simulator can reliably simulate the connections between LEGO bricks. Thus, all robot skills are reduced to deterministic operations when evaluated in simulation, and any variations are due to the stochasticity of planning in APEX-MR.

**Dataset** We evaluate the performance of APEX-MR on a suite of nine LEGO assembly tasks as shown in Fig. 6. The complexity of these tasks varies significantly in terms of the number of objects in the assembly plan, stability, orientation, and manipulation skills required for physical assembly. The Chair shown in Fig. 6(f) has 258 objects, but the structure is solid and stable, and thus, no collaborative skills are needed. On the other hand, many of the bricks along the span of the Bridge (Fig. 6(d)) require a robot to support them when assembling from the top, whereas building the Cliff (Fig. 6(a))

and Faucet (Fig. 6(c)) requires an object reorientation and collaborative assembly from bottom.

**Metrics** We use the execution makespan and wait time as our evaluation metrics for plan quality. Since our output is a TPG, we first roll out the asynchronous trajectory from the TPG, assuming no controller delay. The rollout trajectory converts each pose node back to a configuration. Actions in the skill nodes are executed based on the reference trajectory, and force feedback is switched off in the simulation. The timestamp for each configuration in the rollout trajectory is the earliest possible time to reach this node based on incoming type-2 edges. Execution makespan is the maximum time taken among all robots to execute a trajectory, *i.e.*,  $\max_{i=1}^N t_{N_{end}^i}$ . Wait time is defined as the total amount of time any robot spends waiting in the rollout asynchronous trajectory from TPG, or the original sequential or synchronous trajectory. In particular, we are interested in whether TPG processing can successfully reduce wait time when initialized with a sequential task and motion plan.

**Baseline** We also design a baseline for a synchronized task and motion planning as a comparison to APEX-MR.



(a) Cliff. (b) Branched stairs. (c) Faucet.

(d) Vessel. (e) Guitar. (f) RSS.

Fig. 9: Example LEGO structures constructed in real by the dual-arm system.

Although APEX-MR uses a sequential planner for simplicity and efficiency, our TPG can also improve synchronized motion plans which is a common approach in MR-TAMP. Thus, we evaluate the performance improvement of TPG on synchronized plan as well. In this synchronous planner, robots can execute tasks in parallel but must wait for all robots to finish their current task before proceeding to the next set of tasks. We use an algorithm to convert the sequential task plan from APEX-MR to a synchronous task plan. The main idea is to execute the sequential task plan in parallel if executing the next task does not violate inter-robot task dependencies or block tasks scheduled at an earlier time. This process is similar to building a TPG on tasks instead of motions for parallelization. For every robot  $i$  and its task  $\mathcal{T}_m^i$ , the algorithm checks if the intermediate goal pose  $C_{N_{end,m}}^i$  collides with any other intermediate goal pose of robot  $i'$  and task  $\mathcal{T}_{m'}^{i'}$  that satisfies  $m' < m$ . If there exists a collision, then robot  $i$  must wait for robot  $i'$  to complete task  $\mathcal{T}_{m'}^{i'}$  before starting task  $\mathcal{T}_m^i$ . A synchronous task graph can then be generated by combining these calculated dependencies, with existing inter-robot dependencies. Then, composite RRT-Connect is used as the multi-robot motion planner. Synchronous trajectories for tasks executing in parallel are generated by planning all degrees of freedom as a single robot.

**Performance** Fig. 7 shows the quality of the solution of APEX-MR on a variety of tasks. First, the TPG post-processing and applying and shortcut, as described in Sec. IV-C, significantly reduces makespan by 48% and wait time by 85% on average, compared to the initial sequential motion plan at the horizontal dashed line. Compared to the synchronized motion plan, our asynchronous plans from APEX-MR are consistently shorter and have less wait time. When applied to the synchronous plan, TPG also significantly reduces the makespan by 36% and wait time by 77% on

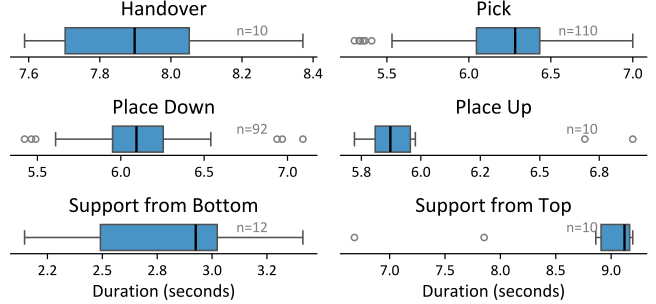


Fig. 10: Distribution of executing various FTS-feedback-controlled LEGO manipulation policy on real robot. The execution time is collected from assembling the Cliff structure in Fig. 9(a) repeatedly. This variation adds to the uncertainty in real-time execution.

average. Note that the post-processed sequential plan from APEX-MR still slightly outperforms the post-processed synchronized motion plan by 3% in terms of makespan. This is due to the path produced by a multi-robot motion plan being suboptimal compared to sequential motion planning. Still, the wait time for the synchronized plan after TPG post-processing is minimal.

**Runtime** Fig. 8 and Table I in the appendix shows the wall clock time for APEX-MR. On average, the TPG construction time is always lower than the task motion planning time except for the Chair, which has a very long assembly sequence. On the other hand, running a synchronized planner can be much more expensive than the simple sequential planner used in APEX-MR, which requires more careful coordination in task planning, and multi-robot motion planning with more degrees of freedom. By combining a simple sequential task and motion planner with TPG post-processing, APEX-MR produces higher-quality multi-robot plans with 26% lower computational overhead on average than a synchronized multi-robot task and motion planner alone.

### B. System Deployment

We deploy the proposed APEX-MR to a real bimanual setup for cooperative LEGO assembly. Fig. 5(b) illustrates the environment setup of the dual-arm system. Note that despite the environment being pre-calibrated, errors ( $\sim 1\text{mm}$ ) still exist since the calibration is imperfect and the structure could be tilted due to the passive connection nature. Thus, we integrate real-time force feedback using the FTS to improve the manipulation robustness. For operation skills (*i.e.*, pick, place-down, place-up, handover), we use the force feedback to detect successful insertion and update the manipulation policy accordingly. For supporting skills (*i.e.*, support-bottom and support-top), we use force feedback to sense a slight touch with the structure to avoid either over or under-supporting. Fig. 9 showcases example LEGO structures accomplished by the bimanual system with APEX-MR. The robots can safely collaborate and efficiently build customized and complex

LEGO objects, including fragile overhanging structures.

Note that the key difference between assembling in real and in simulation is with and without force feedback. Integrating force feedback into the manipulation skills improves the system robustness, but also brings uncertainty with respect to execution time. In particular, we are interested in whether the TPG execution framework ensures safe execution and avoids collisions despite uncertainties from manipulation skills. Fig. 10 depicts the distribution of execution times of six manipulation skills, *i.e.*, pick, place-down, place-up, handover, support-bottom, and support-top (see Fig. 1 for illustrations). All of these skills are designed to execute with force feedback to ensure proper contact between the EOAT and the object being manipulated and minimize the effect of imperfect calibration or tilted structure. As a consequence of these mm-level adjustments with force feedback, the execution time can vary as much as 2 seconds, or as much as 23% from the median. Nevertheless, our TPG execution framework can reliably adjust the robot schedule if any delay could cause a collision or require another robot to wait longer until a skill is completed.

In practice, APEX-MR also allows the two robot arms to operate in close proximity asynchronously thanks to the use of TPG. For example, if one robot is stopped due to a controller issue or because the user presses emergency stop, the other robot would automatically stop if it is unsafe to continue its execution. Although each robot’s feedback controller operates independently, only those actions that are deemed safe are passed to the robot’s action queue. Thus, APEX-MR can significantly reduce the risk of unsafe action in real multi-robot execution.

## VI. LIMITATIONS AND FUTURE WORK

Although the proposed APEX-MR pipeline enables efficient and safe execution for multiple robot arms, it still has several algorithmic limitations which we discuss below.

**Offline Computation** Currently, both the TPG processing and motion planning in APEX-MR are performed offline before real execution. This can be a drawback in real assembly tasks, where new tasks are continuously assigned once the robots finish existing assembly on an assembly line. Another limitation of offline computation is that the APEX-MR cannot adapt to changes in the collision environment or assembly steps easily. A principled framework to address these life-long planning techniques is to use a windowed multi-robot planner and only convert the first  $n$  part of the robot plan to a TPG, similar to how Varambally et al. [59] address automated warehousing. Taking a reduced-horizon approach will significantly reduce planning time and allow plans to be continuously updated concurrently with execution.

**Planning for Robot Dynamics** While APEX-MR are reliable and safe on real robots, APEX-MR requires a good position or force controller for the robot because the generated plan does not consider robot dynamics, such as acceleration and jerk constraints. This is challenging because the planner must generate continuous velocity and acceleration profiles

while also avoiding inter-robot collisions at all times. We plan to incorporate dynamics as part of the TPG post-processing step, such as solving a linear program on top of TPG-imposed constraints and velocity constraints, as suggested in Hönig et al. [20]. Another interesting problem with robot arms is the speed constraints may be imposed on the task space, due to the attached object at the end-effector or even closed kinematic chains formed by concurrent manipulation [60].

**Manipulation Policy** While the proposed APEX-MR enables efficient and safe dual-arm cooperative LEGO assembly, the current system assembles each object based on pre-defined skills. With the additional force feedback, each single operation can be performed robustly. However, due to the passive connection nature of LEGO structures, *i.e.*, established connections could be gradually loosened and the structure can be tilted or even collapse due to subsequent operations, the long-horizon assembly could still fail. Therefore, the dual-arm system, at its current stage, is not robust enough to construct large-scale LEGO structures that have multiple fragile overhanging geometries. To further improve the robustness from a system perspective, we aim to investigate methods for failure detection [4] and recovery, *e.g.*, reinforce the connections that are loosened due to later operations. Failure detection and recovery can also be integrated as part of an online replanning framework that dynamically reschedules the robot’s tasks if a failure occurs and intervention becomes necessary.

**Other Cooperative Assemblies** Building on the APEX-MR pipeline, we plan to extend its application to a broader range of cooperative tasks, such as the NIST Box Assembly [40], and other industrial assembly scenarios. By doing so, we aim to address the unique challenges posed by real-world manufacturing environments, gaining deeper insights into how cooperative systems can be optimized for complex, large-scale production tasks. While the discussion in this paper is based on LEGO assembly, the components in APEX-MR, especially TPG post-processing, can be applied to other multi-robot assembly tasks. A concrete step would be to investigate how to integrate manipulation policies that are more complex than those used for LEGO assembly, *e.g.*, diffusion policy [6], to the TPG framework.

## VII. CONCLUSION

For many robotic manipulation tasks, a team of cooperative robot arms is often necessary and beneficial because cooperation can improve dexterity, flexibility, and versatility. A reliable framework for coordinating robot arms should possess several key qualities: efficiency to maximize throughput, scalability to long-horizon and complex tasks, and safety during real execution.

With these criteria in mind, we have proposed APEX-MR, a pipeline for multi-robot asynchronous planning and execution. Our proposed pipeline combines a sequential task and motion planner with a TPG to post-process the plan for asynchronous execution. Specifically, TPG post-processing can significantly speed up the execution of otherwise sequential and synchronous multi-robot task plans by 48% and 36%

on our simulated assembly tasks. Because coordination is easier, sequential motion planning is far more efficient than planning for synchronous execution.

We demonstrated that our proposed algorithm can be successfully deployed and integrated for a real bimanual cooperative task. LEGO structures, as an example, presented a challenging manipulation task due to the need for high precision and the non-rigid nature of their connections. We presented a set of manipulation skills for complex cooperative assembly, including supported placement and object handover, based on the end-effector design LT-V2. The dual-arm system successfully performs customized LEGO assembly and is the *first* robotic system to do so with commercial LEGO bricks. Additionally, we showed that the integration with the TPG execution framework is robust in the presence of uncertain execution time. In the end, we hope that this framework can advance and bring closer to more real use of multi-robot arm collaboration algorithms.

#### ACKNOWLEDGMENTS

This work is in part supported by the Manufacturing Futures Institute, Carnegie Mellon University, through a grant from the Richard King Mellon Foundation. The authors would also like to thank Yifan Sun for helping design LT-V2.

#### REFERENCES

- [1] Alexander Berndt, Niels Van Duijkeren, Luigi Palmieri, and Tamas Keviczky. A feedback scheme to reorder a multi-agent execution schedule by persistently optimizing a switchable action dependency graph. *arXiv [cs.RO]*, October 2020.
- [2] Z Bien and J Lee. A minimum-time trajectory planning method for two robots. *IEEE Trans. Rob. Autom.*, 8(3): 414–418, June 1992.
- [3] Andrea Brunello, Giuliano Fabris, Alessandro Gasparetto, Angelo Montanari, Nicola Saccomanno, and Lorenzo Scalera. A survey on recent trends in robotics and artificial intelligence in the furniture industry. *Robotics and Computer-Integrated Manufacturing*, 93:102920, 2025. ISSN 0736-5845. doi: <https://doi.org/10.1016/j.rcim.2024.102920>. URL <https://www.sciencedirect.com/science/article/pii/S0736584524002072>.
- [4] Hongyi Chen, Yunchao Yao, Ruixuan Liu, Changliu Liu, and Jeffrey Ichnowski. Automating robot failure recovery using vision-language models with optimized prompts. *arXiv preprint arXiv:2409.03966*, 2024.
- [5] Jingkai Chen, Jiaoyang Li, Yijiang Huang, Caelan Garrett, Dawei Sun, Chuchu Fan, Andreas Hofmann, Caitlin Mueller, Sven Koenig, and Brian C. Williams. Cooperative task and motion planning for multi-arm assembly systems, 2022.
- [6] Cheng Chi, Zhenjia Xu, Siyuan Feng, Eric Cousineau, Yilun Du, Benjamin Burchfiel, Russ Tedrake, and Shuran Song. Diffusion policy: Visuomotor policy learning via action diffusion. *The International Journal of Robotics Research*, 2024.
- [7] David Coleman, Ioan Sucan, Sachin Chitta, and Nikolaus Correll. Reducing the barrier to entry of complex robotic software: a moveit! case study. *arXiv preprint arXiv:1404.3785*, 2014.
- [8] Michael Erdmann and Tomás Lozano-Pérez. On multiple moving objects. *Algorithmica*, 2(1-4):477–521, November 1987.
- [9] Yongxiang Fan, Jieliang Luo, and Masayoshi Tomizuka. A learning framework for high precision industrial assembly. In *2019 International Conference on Robotics and Automation (ICRA)*, page 811–817. IEEE Press, 2019.
- [10] Nigora Gafur, Gajanan Kanagalingam, Achim Wagner, and Martin Ruskowski. Dynamic collision and deadlock avoidance for multiple robotic manipulators. *IEEE Access*, 10:55766–55781, 2022.
- [11] Jonathan D Gammell, Timothy D Barfoot, and Siddhartha S Srinivasa. Batch informed trees (BIT\*): Informed asymptotically optimal anytime search. *Int. J. Rob. Res.*, 39(5):543–567, April 2020.
- [12] K Gao and J Yu. Toward efficient task planning for dual-arm tabletop object rearrangement. *Rep. U. S.*, 2022.
- [13] K Gao, Y Ding, S Zhang, and J Yu. ORLA\*: Mobile manipulator-based object rearrangement with lazy a. *arXiv preprint arXiv:2309.13707*, 2023.
- [14] Kai Gao, Zihe Ye, Duo Zhang, Baichuan Huang, and Jingjin Yu. Toward holistic planning and control optimization for dual-arm rearrangement. April 2024.
- [15] Mokhtar Gharbi, Juan Cortés, and Thierry Siméon. Roadmap composition for multi-arm systems path planning. In *2009 IEEE/RSJ International Conference on Intelligent Robots and Systems*, pages 2471–2476. IEEE, October 2009.
- [16] Kieran Gilday, Josie Hughes, and Fumiya Iida. Achieving flexible assembly using autonomous robotic systems. In *2018 IEEE/RSJ International Conference on Intelligent Robots and Systems (IROS)*, pages 1–9, 2018.
- [17] Kensuke Harada, Tokuo Tsuji, and Jean-Paul Laumond. A manipulation motion planner for dual-arm industrial manipulators. In *2014 IEEE International Conference on Robotics and Automation (ICRA)*, pages 928–934. IEEE, May 2014.
- [18] Valentin Noah Hartmann, Andreas Orthey, Danny Driess, Ozgur S Oguz, and Marc Toussaint. Long-horizon multi-robot rearrangement planning for construction assembly. *arXiv [cs.RO]*, June 2021.
- [19] Wolfgang Honig, Scott Kiesel, Andrew Tinka, Joseph W Durham, and Nora Ayanian. Persistent and robust execution of MAPF schedules in warehouses. *IEEE Robot. Autom. Lett.*, 4(2):1125–1131, April 2019.
- [20] W Hönig, T K Kumar, L Cohen, H Ma, H Xu, and others. Multi-agent path finding with kinematic constraints. *Proceedings of the*, 2016.
- [21] Wolfgang Höning, James A Preiss, T K Satish Kumar,

- Gaurav S Sukhatme, and Nora Ayanian. Trajectory planning for quadrotor swarms. *IEEE Trans. Rob.*, 34(4):856–869, August 2018.
- [22] Daqi Jiang, Hong Wang, and Yanzheng Lu. Mastering the complex assembly task with a dual-arm robot: A novel reinforcement learning method. *IEEE Robot. Autom. Mag.*, 30(2):57–66, June 2023.
- [23] He Jiang, Muhan Lin, and Jiaoyang Li. Speedup techniques for switchable temporal plan graph optimization. In *Proceedings of the AAAI Conference on Artificial Intelligence (AAAI)*, 2025.
- [24] Y Koga and J-C Latombe. On multi-arm manipulation planning. In *Proceedings of the 1994 IEEE International Conference on Robotics and Automation*, pages 945–952 vol.2. IEEE, 1994.
- [25] J J Kuffner and S M LaValle. RRT-connect: An efficient approach to single-query path planning. In *Proceedings 2000 ICRA. Millennium Conference. IEEE International Conference on Robotics and Automation. Symposia Proceedings (Cat. No.00CH37065)*, volume 2, pages 995–1001 vol.2. IEEE, 2000.
- [26] Jiaoyang Li, Wheeler Ruml, and Sven Koenig. Eecbs: A bounded-suboptimal search for multi-agent path finding. In *AAAI Conference on Artificial Intelligence*, pages 12353–12362, 2021.
- [27] Ruixuan Liu, Alan Chen, Xusheng Luo, and Changliu Liu. Simulation-aided learning from demonstration for robotic lego construction. *arXiv preprint arXiv:2309.11010*, 2023.
- [28] Ruixuan Liu, Alan Chen, Weiye Zhao, and Changliu Liu. Physics-aware combinatorial assembly sequence planning using data-free action masking. *arXiv preprint arXiv:2408.10162*, 2024.
- [29] Ruixuan Liu, Kangle Deng, Ziwei Wang, and Changliu Liu. Stablelego: Stability analysis of block stacking assembly. *IEEE Robotics and Automation Letters*, 9(11):9383–9390, 2024. doi: 10.1109/LRA.2024.3414281.
- [30] Ruixuan Liu, Yifan Sun, and Changliu Liu. A Lightweight and Transferable Design for Robust Lego Manipulation. *International Symposium on Flexible Automation*, page V001T07A004, 07 2024. doi: 10.1115/ISFA2024-139981.
- [31] Xusheng Luo, Shaojun Xu, Ruixuan Liu, and Changliu Liu. Decomposition-based hierarchical task allocation and planning for multi-robots under hierarchical temporal logic specifications. *IEEE Robotics and Automation Letters*, 9(8):7182–7189, 2024. doi: 10.1109/LRA.2024.3412589.
- [32] Hang Ma, Jiaoyang Li, T. K. Satish Kumar, and Sven Koenig. Lifelong multi-agent path finding for online pickup and delivery tasks. In *Proceedings of the 16th International Conference on Autonomous Agents and MultiAgent Systems (AAMAS)*, pages 837–845. International Foundation for Autonomous Agents and Multiagent Systems, 2017.
- [33] Hang Ma, T K Satish Kumar, and Sven Koenig. Multi-agent path finding with delay probabilities. *AAAI*, 31(1), February 2017.
- [34] Yusuke Maeda, Ojiro Nakano, Takashi Maekawa, and Shoji Maruo. From cad models to toy brick sculptures: A 3d block printer. In *2016 IEEE/RSJ International Conference on Intelligent Robots and Systems (IROS)*, pages 2167–2172, 2016.
- [35] Tobia Marcucci, Jack Umenberger, Pablo A Parrilo, and Russ Tedrake. Shortest paths in graphs of convex sets. *arXiv [cs.DM]*, January 2021.
- [36] Charles A Meehan, Mark Roberts, and Laura M Hiatt. Asynchronous motion planning and execution for a dual-arm robot. In *Workshop on Planning and Robotics held in conjunction with the International Conference on Automated Planning and Scheduling (ICAPS)*, Virtual, June 2022. URL [https://icaps-conference.org/workshops/PlanRob/papers/PlanRob22\\_paper\\_19.pdf](https://icaps-conference.org/workshops/PlanRob/papers/PlanRob22_paper_19.pdf).
- [37] G. Michalos, S. Makris, N. Papakostas, D. Mourtzis, and G. Chryssolouris. Automotive assembly technologies review: challenges and outlook for a flexible and adaptive approach. *CIRP Journal of Manufacturing Science and Technology*, 2(2):81–91, 2010. ISSN 1755-5817. doi: <https://doi.org/10.1016/j.cirpj.2009.12.001>. URL <https://www.sciencedirect.com/science/article/pii/S1755581709000467>.
- [38] Seyed Sina Mirrazavi Salehian, Nadia Figueroa, and Aude Billard. A unified framework for coordinated multi-arm motion planning. *Int. J. Rob. Res.*, 37(10):1205–1232, September 2018.
- [39] Ludwig Nägele, Alwin Hoffmann, Andreas Schierl, and Wolfgang Reif. Legobot: Automated planning for coordinated multi-robot assembly of lego structures. In *2020 IEEE/RSJ International Conference on Intelligent Robots and Systems (IROS)*, pages 9088–9095, 2020.
- [40] National Institute of Standards and Technology. STEP File Viewer - Box assembly, 2024. URL <https://pages.nist.gov/step-file-viewer.html>.
- [41] Keisuke Okumura and Xavier Défago. Quick multi-robot motion planning by combining sampling and search. *arXiv [cs.RO]*, March 2022.
- [42] Tianyang Pan, Andrew M Wells, Rahul Shome, and Lydia E Kavraki. A general task and motion planning framework for multiple manipulators. In *2021 IEEE/RSJ International Conference on Intelligent Robots and Systems (IROS)*, pages 3168–3174, September 2021.
- [43] Ivaylo Popov, Nicolas Heess, Timothy Lillicrap, Roland Hafner, Gabriel Barth-Maron, Matej Vecerik, Thomas Lampe, Yuval Tassa, Tom Erez, and Martin Riedmiller. Data-efficient deep reinforcement learning for dexterous manipulation. *arXiv*, 2017.
- [44] Yorai Shaoul, Itamar Mishani, Maxim Likhachev, and Jiaoyang Li. Accelerating search-based planning for multi-robot manipulation by leveraging online-generated experiences. In *International Conference on Automated Planning and Scheduling*, 2024.
- [45] Yorai Shaoul, Rishi Veerapaneni, Maxim Likhachev, and

- Jiaoyang Li. Unconstraining multi-robot manipulation: Enabling arbitrary constraints in ecbs with bounded sub-optimality. In *International Symposium on Combinatorial Search*, 2024.
- [46] R Shome and K E Bekris. Synchronized multi-arm rearrangement guided by mode graphs with capacity constraints. *Foundations of Robotics XIV: Proceedings of the ...*, 2021.
- [47] Rahul Shome and Kostas E Bekris. Anytime multi-arm task and motion planning for pick-and-place of individual objects via handoffs. *arXiv [cs.RO]*, May 2019.
- [48] Rahul Shome, Kiril Solovey, Andrew Dobson, Dan Halperin, and Kostas E Bekris. dRRT\*: Scalable and informed asymptotically-optimal multi-robot motion planning. *Auton. Robots*, 44(3):443–467, March 2020.
- [49] Rahul Shome, Kiril Solovey, Jingjin Yu, Kostas Bekris, and Dan Halperin. Fast, high-quality two-arm rearrangement in synchronous, monotone tabletop setups. *IEEE Transactions on Automation Science and Engineering*, 18(3):888–901, 2021. doi: 10.1109/TASE.2021.3055144.
- [50] Christian Smith, Yiannis Karayannidis, Lazaros Nalpanidis, Xavi Gratal, Peng Qi, Dimos V. Dimarogonas, and Danica Kragic. Dual arm manipulation—a survey. *Robotics and Autonomous Systems*, 60(10):1340–1353, 2012. ISSN 0921-8890. doi: <https://doi.org/10.1016/j.robot.2012.07.005>. URL <https://www.sciencedirect.com/science/article/pii/S092188901200108X>.
- [51] Christian Smith, Yiannis Karayannidis, Lazaros Nalpanidis, Xavi Gratal, Peng Qi, Dimos V Dimarogonas, and Danica Kragic. Dual arm manipulation—a survey. *Rob. Auton. Syst.*, 60(10):1340–1353, October 2012.
- [52] Irving Solis, James Motes, Read Sandström, and Nancy M Amato. Representation-optimal multi-robot motion planning using conflict-based search. *IEEE Robotics and Automation Letters*, 6(3):4608–4615, July 2021.
- [53] Kiril Solovey, Oren Salzman, and Dan Halperin. Finding a needle in an exponential haystack: Discrete RRT for exploration of implicit roadmaps in multi-robot motion planning. *Int. J. Rob. Res.*, 35(5):501–513, April 2016.
- [54] Roni Stern, Nathan R. Sturtevant, Ariel Felner, Sven Koenig, Hang Ma, Thayne T. Walker, Jiaoyang Li, Dor Atzmon, Liron Cohen, T. K. Satish Kumar, Eli Boyarski, and Roman Barták. Multi-agent pathfinding: Definitions, variants, and benchmarks. In *Proceedings of the Twelfth Annual Symposium on Combinatorial Search (SoCS)*, pages 151–159, 2019. doi: 10.1609/sochs.v10i1.18510.
- [55] Pascal Stoop, Tharaka Ratnayake, and Giovanni Toffetti. A method for multi-robot asynchronous trajectory execution in MoveIt2. *arXiv [cs.RO]*, October 2023.
- [56] Yifan Su, Rishi Veerapaneni, and Jiaoyang Li. Bidirectional temporal plan graph: Enabling switchable passing orders for more efficient multi-agent path finding plan execution. *arXiv [cs.AI]*, December 2023.
- [57] I. A. Sucan, M. Moll, and L. E. Kavraki. The open motion planning library. *IEEE Robotics and Automation Magazine*, pages 72–82, 2012.
- [58] Yunsheng Tian, Jie Xu, Yichen Li, Jieliang Luo, Shinjiro Sueda, Hui Li, Karl D. D. Willis, and Wojciech Matusik. Assemble them all: Physics-based planning for generalizable assembly by disassembly. *ACM Trans. Graph.*, 41(6), November 2022. ISSN 0730-0301. doi: 10.1145/3550454.3555525. URL <https://doi.org/10.1145/3550454.3555525>.
- [59] Sumanth Varambally, Jiaoyang Li, and Sven Koenig. Which MAPF model works best for automated warehousing? *SOCS*, 15(1):190–198, July 2022.
- [60] Zhou Xian, Puttichai Lertkultanon, and Quang-Cuong Pham. Closed-chain manipulation of large objects by multi-arm robotic systems. *IEEE Robot. Autom. Lett.*, 2(4):1832–1839, October 2017.
- [61] Shiyu Zhang and Federico Pecora. Online and scalable motion coordination for multiple robot manipulators in shared workspaces. *IEEE Trans. Autom. Sci. Eng.*, PP(99):1–20, 2024.

## APPENDIX

### A. Details of Task Planning Formulation

Each assembly step  $a_j$  requires a specific lego type, and each brick in environment has a specific type. Typically, there are many bricks of the same type for in the environment. Mathematically, we represent whether a brick  $b_k$  is the correct type for the assembly step  $a_j$  using a binary variable  $\delta_{j,k}^t$ , where  $\delta_{j,k}^t = 1$  if  $b_k$  is suitable and  $\delta_{j,k}^t = 0$  otherwise. The assembly sequence also specifies whether each step  $a_j$  requires multiple robots for cooperative assembly, denoted by another binary variable  $\delta_j^s$ , where  $\delta_j^s = 1$  if two robots are needed for  $a_j$ .

Let  $X_{ijkg}$  and  $Y_{ijg}$  be the binary decision variables.  $X_{ijkg=1}$  means that robot  $i$  is assigned to assembly step  $j$ , using object  $b_k$  and the  $g^{th}$  grasp pose.  $Y_{ijg}=1$  means that the  $i^{th}$  robot is assigned to support the assembly step  $j$ , using the  $g^{th}$  support pose.  $C_{ijkg}$  and  $C_{ijg}^s$  denote the estimated cost for assigning  $X_{ijkg} = 1$  and  $Y_{ijg} = 1$ , respectively.  $P$  is the maximum number of feasible grasp poses and is set based on the objects and user preferences.  $X_{ijkg} = 1$  means the  $i^{th}$  robot and object  $b_k$  is assigned for the assembly step  $j$ , using the  $g^{th}$  grasp pose. The cost  $C_{ijkg}$  is computed as the sum of joint space distance from robot  $i$ 's HOME pose to  $g^{th}$  robot pose for picking object  $b_k$  to the robot target pose for placing the object at assembly step  $a_j$ . Similarly,  $C_{ijg}^s$  is the distance from robot  $i$ 's HOME pose, to the  $g^{th}$  support pose for step  $a_j$ . The solution to the following ILP program then forms a complete sequential task plan.

$$\arg \min_{X,Y} \sum_{ijk} C_{ijkg} X_{ijkg} + \sum_{ijg} C_{ijg}^s Y_{ijg} + \lambda \sum_j (Z_j^M - Z_j^m) \quad (1)$$

subject to task, robot, and object constraints

The first two terms of optimization minimize the total cost of executing a sequential task plan. The last auxiliary cost term penalizes cases where a single robot is assigned for multiple consecutive tasks and prevents parallelization. The constraints include

$$\sum_{i=1}^N \sum_{k=1}^{N_b} \sum_{g=1}^P X_{ijkg} = 1 \quad \forall j \in [1, \dots, N_a] \quad (2)$$

$$\sum_{i=1}^N \sum_{g=1}^P Y_{ijg} = \delta_j^s \quad \forall j \quad (3)$$

$$\sum_{k=1}^{N_b} \sum_{g=1}^P X_{ijkg} + \sum_{g=1}^P Y_{ijg} \leq 1 \quad \forall i \in [1, \dots, N], \forall j \quad (4)$$

$$\sum_{i=1}^N \sum_{k=1}^{N_b} \sum_{g=1}^P X_{ijkg} \delta_{jk}^t = 1 \quad \forall j \quad (5)$$

$$\sum_{i=1}^N \sum_{j=1}^{N_a} \sum_{g=1}^P X_{ijkg} \leq 1 \quad \forall k \in [1, \dots, N_b] \quad (6)$$

Eqn. 2 ensures that each task is assigned exactly one primary robot. Eqn. 3 assigns a second support robot for each assembly step that needs one. Eqn. 4 prevents each robot from being the primary robot and the support robot at the same step. Eqn. 5 matches an object of the correct type for each assembly step. Eqn. 6 ensures that each object is used at most once. Additionally, the following constraints apply to the auxiliary variables  $\forall i \in [1, \dots, N]$  and  $\forall j = [1, \dots, N_a - N + 1]$

$$z_{i,j} = \sum_{j'=j}^{j+N} \sum_{k=1}^{N_b} \sum_{g=1}^P X_{ij'kg} + \sum_{j'=j}^{j+N} \sum_{g=1}^P Y_{ij'g} \quad (7)$$

$$Z_j^M \geq z_{i,j}, \quad Z_j^m \leq z_{i,j} \quad (8)$$

$z_{ij}$  denotes the number of tasks assigned to robot  $i$  from the task window  $a_j$  to  $a_{j+N-1}$ , whereas  $Z_j^M$  and  $Z_j^m$  are the maximum and minimum  $z_{ij}$  at each window for all robot  $i$ .

### B. Details of Lego Manipulation Policy

### C. Numerical Results

Table I shows the wall clock time for planning, TPG construction, and shortcircuiting across environments averaged over 4 random seeds.

TABLE I: Wall clock time for planning, TPG construction, and shortcuttering across environments (mean  $\pm$  std)

# Objects	Version	Cliff 11	Branched Stairs 14	Faucet 14	Bridge 38	Fish 29	Chair 258	Vessel 36	Guitar 24	RSS 47
Task Planning	APEX-MR	<b>0.6 <math>\pm</math> 0.0</b>	<b>1.1 <math>\pm</math> 0.0</b>	<b>1.1 <math>\pm</math> 0.0</b>	<b>9.7 <math>\pm</math> 0.5</b>	<b>6.5 <math>\pm</math> 0.2</b>	<b>13.0 <math>\pm</math> 0.2</b>	<b>4.9 <math>\pm</math> 0.6</b>	<b>2.3 <math>\pm</math> 0.1</b>	<b>14.5 <math>\pm</math> 0.5</b>
	Sync	1.5 $\pm$ 0.0	1.9 $\pm$ 0.0	2.3 $\pm$ 0.0	10.8 $\pm$ 0.5	8.8 $\pm$ 0.2	27.1 $\pm$ 0.3	6.7 $\pm$ 0.5	3.9 $\pm$ 0.0	18.1 $\pm$ 0.5
Motion Planning	APEX-MR	<b>11.9 <math>\pm</math> 0.3</b>	<b>14.7 <math>\pm</math> 0.3</b>	<b>14.3 <math>\pm</math> 0.2</b>	<b>52.9 <math>\pm</math> 0.8</b>	<b>37.8 <math>\pm</math> 0.6</b>	<b>220.3 <math>\pm</math> 3.5</b>	<b>30.5 <math>\pm</math> 0.7</b>	<b>20.2 <math>\pm</math> 0.1</b>	<b>72.5 <math>\pm</math> 4.6</b>
	Sync	26.7 $\pm$ 0.5	36.4 $\pm$ 1.2	37.2 $\pm$ 0.5	124.8 $\pm$ 2.8	96.7 $\pm$ 1.0	501.9 $\pm$ 5.7	77.4 $\pm$ 0.8	46.8 $\pm$ 0.3	180.9 $\pm$ 7.6
TPG Construction	APEX-MR	<b>9.1 <math>\pm</math> 0.0</b>	<b>9.6 <math>\pm</math> 0.1</b>	<b>10.3 <math>\pm</math> 0.1</b>	35.7 $\pm$ 0.6	29.2 $\pm$ 0.1	<b>341.9 <math>\pm</math> 1.4</b>	<b>16.2 <math>\pm</math> 0.8</b>	<b>16.7 <math>\pm</math> 0.1</b>	<b>52.2 <math>\pm</math> 0.4</b>
	Sync	9.4 $\pm$ 0.2	9.7 $\pm$ 0.0	10.7 $\pm$ 0.3	<b>30.0 <math>\pm</math> 0.6</b>	<b>27.0 <math>\pm</math> 0.2</b>	345.5 $\pm$ 4.3	16.8 $\pm$ 0.2	16.8 $\pm$ 0.0	53.8 $\pm$ 1.0
Total Planning	APEX-MR	<b>21.6 <math>\pm</math> 0.4</b>	<b>25.3 <math>\pm</math> 0.4</b>	<b>25.7 <math>\pm</math> 0.2</b>	<b>98.2 <math>\pm</math> 1.8</b>	<b>73.5 <math>\pm</math> 0.9</b>	<b>575.2 <math>\pm</math> 5.1</b>	<b>51.6 <math>\pm</math> 2.1</b>	<b>9.2 <math>\pm</math> 0.2</b>	<b>139.3 <math>\pm</math> 5.5</b>
	Sync	37.5 $\pm$ 0.8	48.0 $\pm$ 1.2	50.1 $\pm$ 0.8	165.6 $\pm$ 3.8	132.5 $\pm$ 1.4	874.6 $\pm$ 10.3	100.9 $\pm$ 1.5	67.5 $\pm$ 0.3	252.8 $\pm$ 9.1
TPG Shortcut		20	20	20	20	20	60	60	60	60